Intermolecular Charge Transfer Induced Fragmentation of Formic Acid Dimers

Jiaqi Zhou,[1] Shaokui Jia,[1] Xiaoqing Hu,[2,*] Enliang Wang,[3] Xiaorui Xue,[1] Yong Wu,[2,†] Jianguo Wang,[2] Alexander Dorn,[4] and Xueguang Ren[1,‡]

[1]*School of Physics, Xi'an Jiaotong University, Xi'an 710049, China*
[2]*Institute of Applied Physics and Computational Mathematics, Beijing 100088, China*
[3]*Hefei National Laboratory for Physical Sciences at the Microscale and Department of Modern Physics, University of Science and Technology of China, Hefei 230026, China*
[4]*Max-Planck-Institut für Kernphysik, Saupfercheckweg 1, 69117 Heidelberg, Germany*

(Received 9 November 2022; revised 19 January 2023; accepted 20 April 2023; published 7 June 2023)

We investigate the intermolecular nonradiative charge transfer process in a double hydrogen-bonded formic acid (FA) dimer, initiated by electron-collision induced double ionization of one FA molecule. Through fragment ions and electron coincident momentum measurements and *ab initio* calculations, we obtain direct evidence that electron transfer from the neighboring FA molecule to fill one of the two vacancies occurs by a potential energy curve crossing of $FA^{++} + FA$ with $FA^{+} + FA^{+*}$ curves, forming an electronic excited state of dicationic dimers. This process causes the breaking of two hydrogen bonds and subsequently the cleavage of C—H and C—O covalent bonds in the dimers, which is expected to be a general phenomenon occurring in molecular complexes and can have important implications for radiation damage to biological matter.

DOI: 10.1103/PhysRevLett.130.233001

Charge transfer (CT) between molecules is a key process in many areas of physics, chemistry, biology, and materials science [1–7]. It contributes substantially to the properties and dynamics of molecular systems at the microscopic level, which are essential for the fundamental understanding of phenomena ranging from photosynthesis to DNA damage [6–10]. In recent years, studying the relaxation properties of molecular aggregates in their electronic excited states has attracted a growing interest due to the discovery of a wealth of new energy and charge transfer processes, notably intermolecular Coulombic decay (ICD) [11] and electron transfer mediated decay (ETMD) [12].

In ICD, an inner-valence vacancy is filled by an outer-valence electron from the same site and the energy released is transferred in a femtosecond timescale to ionize a neighboring molecule [13,14]. In ETMD, the initial vacancy is not filled locally, but by electron transfer from a neighboring site that leads to the emission of a low-energy electron from either the donor itself or another neighboring species [15–21]. The latter process has been identified in heterogeneous NeKr clusters involving a $Ne(2p^{-2})$ dication [20,21], where a $4p$ electron of Kr is transferred to fill one of the two vacancies in $Ne(2p^{-2})$, causing ionization of another neutral Kr atom in the vicinity. This relaxation path, however, is energetically not favorable for the homogeneous systems. Instead, a radiative charge transfer (RCT) process may occur in which the energy released upon neutralization of the dication is emitted as a photon [22–26]. However, a recent study suggested that RCT is efficiently quenched by nonradiative CT in mixed ArN_2 clusters. This direct CT process can proceed because there exists a manifold of excited N_2^{+*} states, which intersect with the one-site dicationic states [27].

In the present Letter, we address the question whether such direct CT can be a general pathway for the fragmentation of molecules in more complex biological systems, which remains largely unexplored. The biological analog studied here is the formic acid (FA, HCOOH) dimer, which forms dominantly an eight-membered ring structure with a double hydrogen bond [Fig. 1(d)] [28,29]. This dimer is closely related to biological systems like hydrogen-bonded DNA base pairs [30–37].

We consider the double ionization of a FA dimer and subsequent reaction pathway induced by electron impact ($E_0 = 90$ eV). An important motivation of this Letter is that the low-energy electron-initiated processes are found to be responsible for an essential part of the radiation effects in gases and condensed matter [38–40]. As is illustrated in Fig. 1, the reaction can be divided into three steps. In step 1, two outer-valence electrons from one molecule of the dimer are ionized by electron impact (one-site double ionization), forming a $FA^{++} \cdot FA$ state [Fig. 1(a)],

$$e^- + FA \cdot FA \rightarrow 3 \times e^- + FA^{++} \cdot FA. \quad (1)$$

We notice here that photoionization process is also possible to create such a one-site dicationic dimer, e.g., by direct double photoionization or through intramolecular Auger decay [41,42]. In step 2, an outer-valence electron from the neighboring site is transferred to fill one of the two

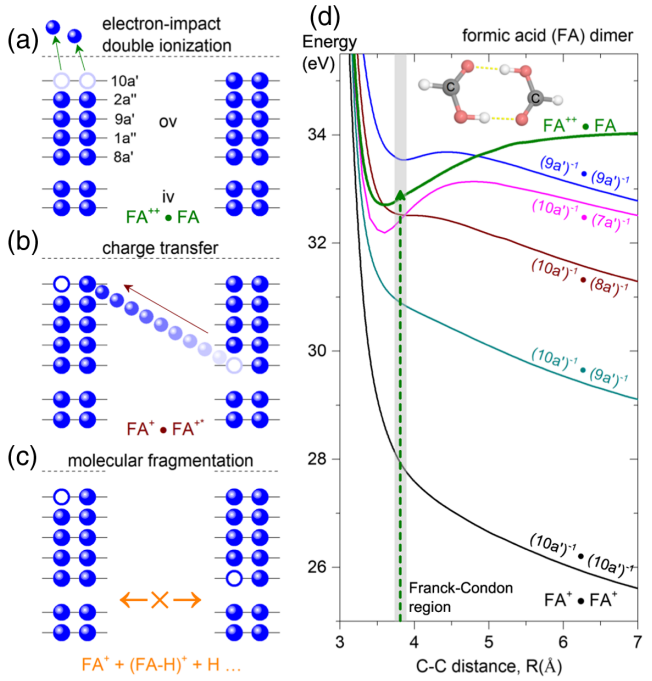

FIG. 1. Illustration of direct CT in FA dimers. (a) Two outer-valence (ov) vacancies are initially created on one site of the dimer upon electron impact, which forms a $FA^{++} \cdot FA$ dicationic dimer. (b) One of the two vacancies is filled by an electron from the neighboring site. This process occurs by a PEC crossing of the $FA^{++} + FA$ curve with a $FA^{+} + FA^{+*}$ curve. (c) As a result, the dimer fragments with a Coulomb explosion pathway and subsequent neutral dissociation. (d) Calculated PECs of one-site dicationic ground state ($FA^{++} \cdot FA$) and two-site dicationic ground ($FA^{+} \cdot FA^{+}$) and various excited state dimers as a function of C-C distance using the CASSCF method [27].

vacancies. This process occurs by a potential energy curve (PEC) crossing of the $FA^{++} + FA$ curve with a $FA^{+} + FA^{+*}$ curve where the molecule is electronically excited [27] [Fig. 1(b)],

$$FA^{++} \cdot FA \rightarrow FA^{+} \cdot FA^{+*}. \quad (2)$$

In step 3, the system relaxes by Coulomb explosion and further dissociation processes [Fig. 1(c)],

$$FA^{+} \cdot FA^{+*} \rightarrow FA^{+} + FA^{+*}(H + COOH^{+}, \ldots). \quad (3)$$

The PECs for the doubly ionized states of FA dimers are presented in Fig. 1(d) as a function of C-C distance, which are calculated using the complete active space self-consistent field method (CASSCF) method [43–45]. Below, we confirm the dissociation pathway by fragment ions and electron coincident momentum spectroscopy as well as *ab initio* molecular dynamics (AIMD) simulation.

Our experiments were carried out using a multiparticle momentum spectrometer with a pulsed photoemission electron source [46–48]. The fragmentation of FA dimers are studied by triple-coincidence detection of two fragment ions and one outgoing electron (see Supplemental Material [49]). The three-dimensional momentum vectors for all detected particles as well as the mass-over-charge ratios of the ions are determined. For each detected ion pair, we obtain the related projectile energy-loss (E_{loss}) spectrum, which can provide insight into the ionization mechanism of the reaction [29].

We identify the fragmentation channels using a time-correlation map between two fragment ions, which is shown in Fig. 2. This map shows several diagonal structures, among them the sharp one (solid line) indicates the dimer fragments into two FA^{+} cations that are emitted back

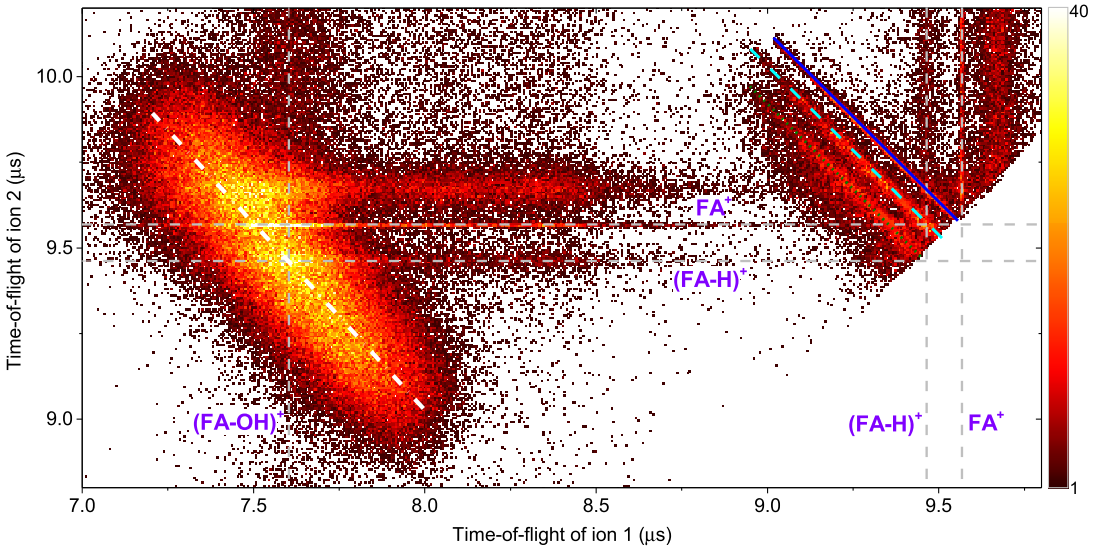

FIG. 2. Measured time-correlation map between two ions. The distributions at the solid, dashed, dotted, and dash-dotted diagonal lines show the breakup of the dicationic dimer into $FA^{+} + FA^{+}$, $FA^{+} + (FA\text{-}H)^{+} + H$, $(FA\text{-}H)^{+} + (FA\text{-}H)^{+} + 2 \times H$, and $(FA\text{-}H)^{+} + H + (FA\text{-}OH)^{+} + OH$ channels.

to back with momenta of equal magnitude but opposite direction. In addition, the dashed, dotted, and dash-dotted diagonal lines indicate the fragmentation channels where some neutral species are emitted during the Coulomb explosion process, i.e., $FA^+ + (FA\text{-}H)^+ + H$ (dashed line), $(FA\text{-}H)^+ + (FA\text{-}H)^+ + 2\times H$ (dotted line), and $(FA\text{-}OH)^+ + OH + (FA\text{-}H)^+ + H$ (dash-dotted line). The width of these correlation structures becomes broader due to the missing momenta of the undetected neutral species. Furthermore, we determine the product ratios as 1:1.8:2.0:32.0 for $[FA^+ + FA^+]$: $[FA^+ + (FA\text{-}H)^+]$: $[(FA\text{-}H)^+ + (FA\text{-}H)^+]$: $[(FA\text{-}OH)^+ + (FA\text{-}H)^+]$ channels, respectively. Compared to the ion yield ratios of FA^+: $(FA\text{-}H)^+$: $(FA\text{-}OH)^+$ in the ionization process of monomers, which are 1:0.8:1.72 [55], we observe an enhancement of the fragmentation yields in the present decay process, particularly for the $(FA\text{-}OH)^+ + (FA\text{-}H)^+$ channel. Experimentally, we have identified that the $FA^+ + FA^+$ Coulomb explosion channel is mainly caused by the ICD mechanism upon inner-valence ionization of one FA molecule with threshold of about 28 eV [29], while the other channels involving neutral dissociation are found to be due to one-site double ionization of the dimer and subsequent nonradiative CT process, which will be discussed below. It should be noted that both ETMD and RCT are minor contributions here because the excess energy is not sufficient to cause further ionization of the homogeneous FA dimer through ETMD [12,15–21], and according to [27] RCT is efficiently quenched by direct CT process.

Figure 3 shows the projectile E_{loss} spectra related to the different ion pairs. The threshold energy leading to specific ionization products can be determined from the onsets of the measured E_{loss} spectra, e.g., the $E_{\text{loss}} \sim 24.5$ eV is obtained for the ionization of He that is used for calibration (solid curve in Fig. 3). For all three fragmentation channels, we determine the E_{loss} to be roughly 32.5–33.0 eV, which is in line with the double-ionization threshold of the FA monomer (33.08 eV) computed using the coupled cluster singles, doubles, and perturbative triples theory and the aug-cc-pVTZ level basis set (vertical dashed line). This E_{loss} is higher by about 5.0 eV than the calculated double-ionization threshold of the FA dimer (vertical dash-dotted line), which amounts to around 28 eV, corresponding to the electronic ground state of the dicationic $FA^+ \cdot FA^+$ dimer. The obtained E_{loss} indicates that these fragmentation processes are initiated by one-site double ionization of the dimer, forming a $FA^{++} \cdot FA$ state. Further electron transfer between the molecules involving a PEC crossing leads to the formation of a two-site dicationic excited state like $(10a')^{-1} \cdot (8a')^{-1}$ [Fig. 1(d)]. The molecule can further dissociate into different ionic and neutral species depending on the internal energy and ionization state [37,55,56].

To quantify the fragmentation processes, we have performed AIMD simulations starting from the sampled neutral dimers with a given initial temperature (30 K) and vertical

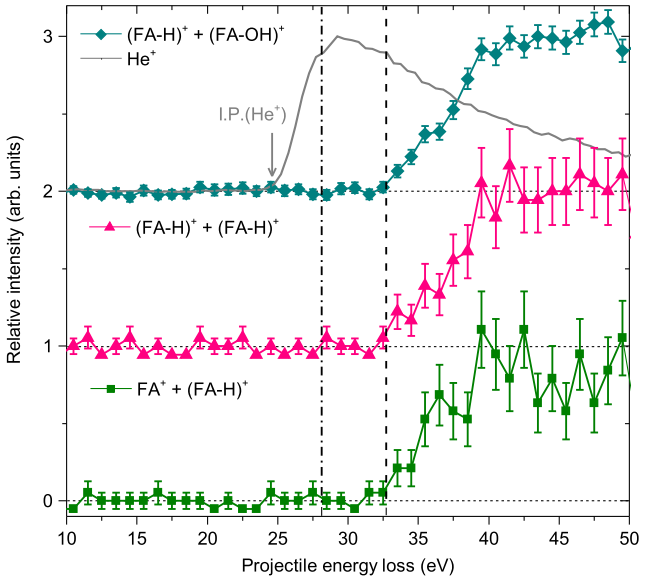

FIG. 3. Projectile energy loss spectra. The distributions show the results for the double ionization of FA dimers leading to $FA^+ + (FA\text{-}H)^+ + H$, $(FA\text{-}H)^+ + (FA\text{-}H)^+ + 2\times H$ and $(FA\text{-}H)^+ + H + (FA\text{-}OH)^+ + OH$ channels. Also included is the spectrum for the single ionization of helium atom (He^+). I.P., ionization potential. Vertical dashed and dash-dotted lines represent the double-ionization thresholds of the FA monomer and dimer, respectively.

transition to the two-site doubly charged $FA^+ \cdot FA^+$ dimer [57,58]. Here we further impart an amount of internal energy (0.2 hartree) into the system to consider approximately the electronic excited state of the two-site dicationic dimer. The amount of internal energy is adapted to the measured E_{loss} spectra shown in Fig. 3. Our calculations were performed using an atom-centered density matrix propagation method with the long-ranged density-functional theory at the ωB97XD/cc-pVTZ level (see Supplemental Material [49]). We note that the dimer dynamics before the CT process like the reduction of the intermolecular separation are neglected in the present calculations. Further, the internal electronic excitation energy is assumed to be converted into vibrational thermal energy (internal conversion).

For the fragmentation channel of $FA^+ + (FA\text{-}H)^+ + H$, the measured and calculated kinetic energy release (KER) spectra are presented in Fig. 4(a). Here, the kinetic energy (KE) for the neutral H is reconstructed from momentum conservation. Our AIMD simulations reproduce very well the center value (KER ~ 4.5 eV) of the measured KER peak. The width of the predicted KER peak is narrow in comparison with the experimental spectrum due to the possible nuclear dynamics occurring before the PEC crossing, which are not considered in the simulations. Our calculations indicate that after the relaxation process the dicationic dimer starts to explode into two FA^+ cations with a direct breaking of the double hydrogen bond [Fig. 4(c)]. During the explosion, one of the C—H bonded

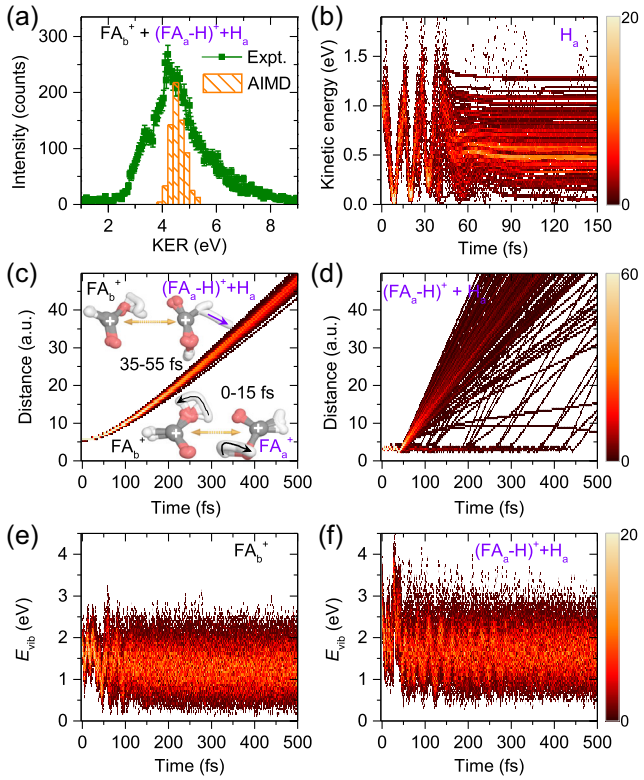

FIG. 4. Fragmentation dynamics of the dicationic dimer into $FA^+ + (FA\text{-}H)^+ + H$ pathway. (a) Measured KER spectrum in comparison to AIMD calculation. (b)–(f) The AIMD calculated results as a function of propagation time for the KE of C—H bonded H atoms (b); The center-of-mass distance $R_{c.m.}$ between (c) FA^+ and $(FA\text{-}H)^+ + H$ and between (d) $(FA\text{-}H)^+$ and neutral H. The E_{vib} for the (e) nondissociative FA^+ cation and the (f) dissociative ion $FA^+ \rightarrow (FA\text{-}H)^+ + H$. The insets in (c) show the path-integral trajectories in the time range of 0-15 and 35–55 fs.

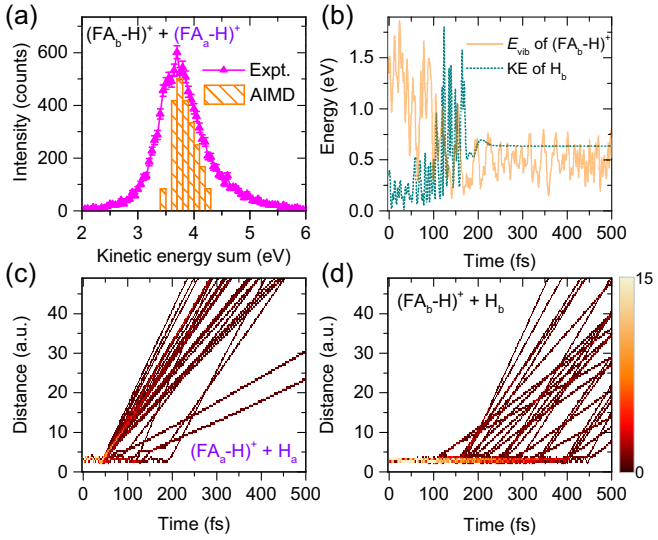

FIG. 5. Fragmentation dynamics of the dicationic dimer into $(FA\text{-}H)^+ + (FA\text{-}H)^+ + 2 \times H$ pathway. (a) Measured and AIMD calculated kinetic energy sum spectrum of $(FA\text{-}H)^+ + (FA\text{-}H)^+$ ion pair. (b) The calculated KE of C—H bonded H atom (dotted line) and the E_{vib} of $(FA\text{-}H)^+$ group (solid line) for one typical trajectory of the second H-loss channel. The calculated $R_{c.m.}$ between $(FA\text{-}H)^+$ and neutral H for the (c) first and (d) second H-loss channels.

H atoms (H_a) undergoes fast and strong vibrational motions, see the KE spectrum of H_a in Fig. 4(b). In addition, it can be seen from the center-of-mass (c.m.) distance spectrum in Fig. 4(d) that the H_a atom starts to dissociate from the FA_a^+ cation at about 50 fs, which is also visible from the path-integral trajectories (35–55 fs) shown in the insets of Fig. 4(c). Our calculations reveal that the hydrogen loss (H-loss) process is caused by the increased internal vibration energy (E_{vib}) of FA_a^+ particularly at $t \sim 50$ fs [Fig. 4(f)] in comparison to that of the nondissociative FA_b^+ cations [Fig. 4(e)].

In the double H-loss process, i.e., $(FA\text{-}H)^+ + (FA\text{-}H)^+ + 2H$ channel, the kinetic energy sum of the $(FA\text{-}H)^+ + (FA\text{-}H)^+$ ion pair is provided in Fig. 5(a), which is also compared with the AIMD calculations. Both spectra show very good agreement with each other, which display a single-peak structure centered at about 3.75 eV. Our calculations indicate that, during the Coulomb explosion, two C—H bonded H atoms tend to dissociate subsequently from each of the FA^+ cations. As shown in Fig. 5(c), a fast H-loss process occurs with a high probability at about 50 fs, in which the formation mechanisms are essentially similar to the aforementioned H-loss process (Fig. 4), while in the second H-loss process, the KE of the C—H bonded H atom (dotted line in Fig. 5(b)] is initially too low to activate the H-loss process. We found that an amount of the internal energy is transferred gradually from the E_{vib} of the $(FA\text{-}H)^+$ group [solid line in Fig. 5(b)] to the KE of the H atom. This leads to the final dissociation of FA^+ into $(FA\text{-}H)^+$ and H atom at the later times ($t > 100$ fs), see Fig. 5(d). More dynamical trajectories are presented in Fig. 2 of the Supplemental Material [49]. Similar results are also obtained for the fragmentation dynamics of $(FA\text{-}OH)^+ + OH + (FA\text{-}H)^+ + H$ channel, where the C—O bond breaking and OH abstraction are found to be caused by the increased KE of OH species (see Supplemental Material [49]).

To summarize, our studies of nonradiative charge transfer between FA molecules reveal an efficient pathway for fragmentation of molecular complexes induced by low-energy electron impact. This intermolecular relaxation process is initiated by the removal of two outer-valence electrons from one site of the dimer, which is followed by direct CT through a PEC crossing of $FA^{++} + FA$ with $FA^+ + FA^{+*}$ curves. This leads to the formation of electronic excited states of dicationic dimers, undergoing Coulomb explosion and molecular fragmentation. The occurrence of the direct CT process is proved by determining the initial state as a charge-localized $FA^{++} \cdot FA$

dicationic state from the correlated projectile energy loss spectra. Our studies demonstrate that even ground state dications can further decay by direct CT involving with a neighboring molecule, which is fundamentally distinct from the ICD mechanism [11,13,14]. This Letter provides a new route to experimentally separate ICD and direct CT with the determinations of the initial electronic states.

The fragmentation dynamics of FA dimers following direct CT were well described by the AIMD calculations, which indicate that the two hydrogen bonds are broken once the CT process occurs in the dimers, resulting in two FA^+ ions. Depending on the internal energy or the ionization state, the C—H and C—O covalent bonds are further cleaved in the timescale of about 50–100 fs. The present results could have important consequences for radiation damage to biological tissues both for the fundamental reason of generating various radicals and because of the chemical bond breaking caused by this direct CT process. Furthermore, we found that direct CT can lead to a significant enhancement of fragmentation yields (~36 times higher than ICD in the FA dimers), and the abundant reactive radicals can constitute more severe local damage in the biological system, which has not been considered previously. The present observation is expected to be a general phenomenon occurring in radiation biology and chemistry where the dication can be created directly by the ionizing radiations like x rays, neutrons, and swift ions or indirectly through collision with the secondary electrons [38–40]. Indeed, our further calculations indicate that it may also occur in the complex system involving a Mg^{++} dication in the electronic ground state and a neutral glycine leading to the C—C bond breaking of the molecule (see Supplemental Material [49]), where glycine is the simplest prototype of the amino acids commonly found in proteins and the metal ions like Mg^{++} are essential for living organisms [59–61]. We note that the present observation is not limited to dications, but similar processes will also take place upon multiple ionization of the high-Z atoms in the human body, e.g., by x-ray irradiation [59–61], leading to extensive local damage to biomolecules.

This work was supported by the National Natural Science Foundation of China under Grants No. 92261201, No. 11974272, No. 11934004, and No. 12104063. E. W. is grateful for support from the Strategic Priority Research Program of Chinese Academy of Sciences, Grant No. XDB34020000.

J. Z. and S. J. contributed equally to this work.

*xiaoqing-hu@foxmail.com
†wu_yong@iapcm.ac.cn
‡renxueguang@xjtu.edu.cn

[1] R. A. Marcus, Electron transfer reactions in chemistry. Theory and experiment, Rev. Mod. Phys. **65**, 599 (1993).
[2] B. Erk *et al.*, Imaging charge transfer in iodomethane upon x-ray photoabsorption, Science **345**, 288 (2014).
[3] X. Hong, J. Kim, S.-F. Shi, Y. Zhang, C. Jin, Y. Sun, S. Tongay, J. Wu, Y. Zhang, and F. Wang, Ultrafast charge transfer in atomically thin MoS_2/WS_2 heterostructures, Nat. Nanotechnol. **9**, 682 (2014).
[4] J.-L. Brédas, D. Beljonne, V. Coropceanu, and J. Cornil, Charge-transfer and energy-transfer processes in π-conjugated oligomers and polymers: A molecular picture, Chem. Rev. **104**, 4971 (2004).
[5] S. Rafiq, B. Fu, B. Kudisch, and G. D. Scholes, Interplay of vibrational wavepackets during an ultrafast electron transfer reaction, Nat. Chem. **13**, 70 (2021).
[6] V. May and O. Kühn, *Charge and Energy Transfer Dynamics in Molecular Systems* (John Wiley & Sons, New York, 2011).
[7] H. J. Wörner *et al.*, Charge migration and charge transfer in molecular systems, Struct. Dyn. **4**, 061508 (2017).
[8] D. B. Hall, R. E. Holmlin, and J. K. Barton, Oxidative DNA damage through long-range electron transfer, Nature (London) **382**, 731 (1996).
[9] N. M. Riley and J. J. Coon, The role of electron transfer dissociation in modern proteomics, Anal. Chem. **90**, 40 (2018).
[10] J. Nguyen, Y. Ma, T. Luo, R. G. Bristow, D. A. Jaffray, and Q.-B. Lu, Direct observation of ultrafast-electron-transfer reactions unravels high effectiveness of reductive DNA damage, Proc. Natl. Acad. Sci. U.S.A. **108**, 11778 (2011).
[11] L. S. Cederbaum, J. Zobeley, and F. Tarantelli, Giant Intermolecular Decay and Fragmentation of Clusters, Phys. Rev. Lett. **79**, 4778 (1997).
[12] J. Zobeley, R. Santra, and L. S. Cederbaum, Electronic decay in weakly bound heteroclusters: Energy transfer versus electron transfer, J. Chem. Phys. **115**, 5076 (2001).
[13] U. Hergenhahn, Interatomic and intermolecular Coulombic decay: The early years, J. Electron Spectrosc. Relat. Phenom. **184**, 78 (2011).
[14] T. Jahnke, U. Hergenhahn, B. Winter, R. Dörner, U. Frühling, P. V. Demekhin, K. Gokhberg, L. S. Cederbaum, A. Ehresmann, A. Knie, and A. Dreuw, Interatomic and intermolecular Coulombic decay, Chem. Rev. **120**, 11295 (2020).
[15] M. Förstel, M. Mucke, T. Arion, A. M. Bradshaw, and U. Hergenhahn, Autoionization Mediated by Electron Transfer, Phys. Rev. Lett. **106**, 033402 (2011).
[16] K. Sakai, S. Stoychev, T. Ouchi, I. Higuchi, M. Schöffler, T. Mazza, H. Fukuzawa, K. Nagaya, M. Yao, Y. Tamenori, A. I. Kuleff, N. Saito, and K. Ueda, Electron-Transfer-Mediated Decay and Interatomic Coulombic Decay from the Triply Ionized States in Argon Dimers, Phys. Rev. Lett. **106**, 033401 (2011).
[17] I. Unger, R. Seidel, S. Thürmer, M. N. Pohl, E. F. Aziz, L. S. Cederbaum, E. Muchová, P. Slavíček, B. Winter, and N. V. Kryzhevoi, Observation of electron-transfer-mediated decay in aqueous solution, Nat. Chem. **9**, 708 (2017).
[18] L. Ben Ltaief, M. Shcherbinin, S. Mandal, S. R. Krishnan, R. Richter, T. Pfeifer, M. Bauer, A. Ghosh, M. Mudrich, K. Gokhberg, and A. C. LaForge, Electron transfer mediated decay of alkali dimers attached to he nanodroplets, Phys. Chem. Chem. Phys. **22**, 8557 (2020).

[19] A. Ghosh, L. S. Cederbaum, and K. Gokhberg, Signature of the neighbor's quantum nuclear dynamics in the electron transfer mediated decay spectra, Chem. Sci. **12**, 9379 (2021).

[20] V. Stumpf, P. Kolorenč, K. Gokhberg, and L. S. Cederbaum, Efficient Pathway to Neutralization of Multiply Charged Ions Produced in Auger Processes, Phys. Rev. Lett. **110**, 258302 (2013).

[21] D. You *et al.*, Charge transfer to ground-state ions produces free electrons, Nat. Commun. **8**, 14277 (2017).

[22] N. Saito, Y. Morishita, I. H. Suzuki, S. D. Stoychev, A. I. Kuleff, L. S. Cederbaum, X.-J. Liu, H. Fukuzawa, G. Prümper, and K. Ueda, Evidence of radiative charge transfer in argon dimers, Chem. Phys. Lett. **441**, 16 (2007).

[23] K. Kreidi *et al.*, Relaxation processes following 1*s* photoionization and Auger decay in Ne_2, Phys. Rev. A **78**, 043422 (2008).

[24] S. D. Stoychev, A. I. Kuleff, F. Tarantelli, and L. S. Cederbaum, On the interatomic electronic processes following Auger decay in neon dimer, J. Chem. Phys. **129**, 074307 (2008).

[25] X. Ren, E. Jabbour Al Maalouf, A. Dorn, and S. Denifl, Direct evidence of two interatomic relaxation mechanisms in argon dimers ionized by electron impact, Nat. Commun. **7**, 11093 (2016).

[26] A. Hans, V. Stumpf, X. Holzapfel, F. Wiegandt, P. Schmidt, C. Ozga, P. Reiß, L. B. Ltaief, C. Küstner-Wetekam, T. Jahnke, A. Ehresmann, P. V. Demekhin, K. Gokhberg, and A. Knie, Direct evidence for radiative charge transfer after inner-shell excitation and ionization of large clusters, New J. Phys. **20**, 012001 (2018).

[27] C. Küstner-Wetekam, X. Q. Hu, L. Marder, P. Schmidt, C. Ozga, C. Zindel, H. Otto, Y. G. Peng, J. G. Wang, C. Richter, N. Sisourat, U. Hergenhahn, A. Knie, A. Ehresmann, Y. Wu, and A. Hans, Nature and impact of charge transfer to ground-state dications in atomic and molecular environments, Phys. Rev. A **104**, 042802 (2021).

[28] J. Chocholoušová, J. Vacek, and P. Hobza, Potential energy and free energy surfaces of the formic acid dimer: Correlated *ab initio* calculations and molecular dynamics simulations, Phys. Chem. Chem. Phys. **4**, 2119 (2002).

[29] J. Zhou, S. Jia, A. D. Skitnevskaya, E. Wang, T. Hähnel, E. K. Grigoricheva, X. Xue, J.-X. Li, A. I. Kuleff, A. Dorn, and X. Ren, Concerted double hydrogen-bond breaking by intermolecular Coulombic decay in the formic acid dimer, J. Phys. Chem. Lett. **13**, 4272 (2022).

[30] M. Allan, Electron Collisions with Formic Acid Monomer and Dimer, Phys. Rev. Lett. **98**, 123201 (2007).

[31] V. V. Matylitsky, C. Riehn, M. F. Gelin, and B. Brutschy, The formic acid dimer $(HCOOH)_2$ probed by time-resolved structure selective spectroscopy, J. Chem. Phys. **119**, 10553 (2003).

[32] Ö. Birer and M. Havenith, High-resolution infrared spectroscopy of the formic acid dimer, Annu. Rev. Phys. Chem. **60**, 263 (2009).

[33] S. Scheiner and C. W. Kern, Molecular orbital investigation of multiply hydrogen bonded systems. Formic acid dimer and DNA base pairs, J. Am. Chem. Soc. **101**, 4081 (1979).

[34] K. Hoshina, H. Hagihara, and M. Tsuge, Double ionization and Coulomb explosion of the formic acid dimer by intense near-infrared femtosecond laser pulses, J. Phys. Chem. A **116**, 826 (2012).

[35] J. Novak, M. Mališ, A. Prlj, I. Ljubić, O. Kühn, and N. Došlić, Photoinduced dynamics of formic acid monomers and dimers: The role of the double hydrogen bond, J. Phys. Chem. A **116**, 11467 (2012).

[36] P. Farfán, A. Echeverri, E. Diaz, J. D. Tapia, S. Gómez, and A. Restrepo, Dimers of formic acid: Structures, stability, and double proton transfer, J. Chem. Phys. **147**, 044312 (2017).

[37] M. S. Arruda, A. Medina, J. N. Sousa, L. A. V. Mendes, R. R. T. Marinho, and F. V. Prudente, Communication: Protonation process of formic acid from the ionization and fragmentation of dimers induced by synchrotron radiation in the valence region, J. Chem. Phys. **144**, 141101 (2016).

[38] S. M. Pimblott and J. A. LaVerne, Production of low-energy electrons by ionizing radiation, Radiat. Phys. Chem. **76**, 1244 (2007).

[39] B. C. Garrett *et al.*, Role of water in electron-initiated processes and radical chemistry: Issues and scientific advances, Chem. Rev. **105**, 355 (2005).

[40] E. Alizadeh, T. M. Orlando, and L. Sanche, Biomolecular damage induced by ionizing radiation: The direct and indirect effects of low-energy electrons on DNA, Annu. Rev. Phys. Chem. **66**, 379 (2015).

[41] R. Wehlitz, Double photoionization of hydrocarbons and aromatic molecules, J. Phys. B **49**, 222004 (2016).

[42] A. Hans, P. Schmidt, C. Küstner-Wetekam, F. Trinter, S. Deinert, D. Bloß, J. H. Viehmann, R. Schaf, M. Gerstel, C. M. Saak, J. Buck, S. Klumpp, G. Hartmann, L. S. Cederbaum, N. V. Kryzhevoi, and A. Knie, Suppression of x-ray-induced radiation damage to biomolecules in aqueous environments by immediate intermolecular decay of inner-shell vacancies, J. Phys. Chem. Lett. **12**, 7146 (2021).

[43] H.-J. Werner *et al.*, MOLPRO, version 2010.1, a package of *ab initio* programs, http://www. molpro.net.

[44] H.-J. Werner, P. J. Knowles, G. Knizia, F. R. Manby, and M. Schütz, MOLPRO: A general-purpose quantum chemistry program package, WIREs Comput. Mol. Sci. **2**, 242 (2012).

[45] P. J. Knowles and H.-J. Werner, An efficient second-order MC SCF method for long configuration expansions, Chem. Phys. Lett. **115**, 259 (1985).

[46] J. Ullrich, R. Moshammer, A. Dorn, R. Dörner, L. Schmidt, and H. Schmidt-Böcking, Recoil-ion and electron momentum spectroscopy: Reaction-microscopes, Rep. Prog. Phys. **66**, 1463 (2003).

[47] X. Ren, T. Pflüger, M. Weyland, W. Y. Baek, H. Rabus, J. Ullrich, and A. Dorn, An $(e, 2e + \text{ion})$ study of low-energy electron-impact ionization and fragmentation of tetrahydrofuran with high mass and energy resolutions, J. Chem. Phys. **141**, 134314 (2014).

[48] X. Ren, E. Wang, A. D. Skitnevskaya, A. B. Trofimov, K. Gokhberg, and A. Dorn, Experimental evidence for ultrafast intermolecular relaxation processes in hydrated biomolecules, Nat. Phys. **14**, 1062 (2018).

[49] See Supplemental Material at http://link.aps.org/supplemental/10.1103/PhysRevLett.130.233001 for technical and calculational details, which includes Refs. [50–54].

[50] H. B. Schlegel, J. M. Millam, S. S. Iyengar, G. A. Voth, A. D. Daniels, G. E. Scuseria, and M. J. Frisch, *Ab initio* molecular dynamics: Propagating the density matrix with Gaussian orbitals, J. Chem. Phys. **114**, 9758 (2001).

[51] S. S. Iyengar, H. B. Schlegel, J. M. Millam, G. A. Voth, G. E. Scuseria, and M. J. Frisch, *Ab initio* molecular dynamics: Propagating the density matrix with Gaussian orbitals. II. Generalizations based on mass-weighting, idempotency, energy conservation and choice of initial conditions, J. Chem. Phys. **115**, 10291 (2001).

[52] H. B. Schlegel, S. S. Iyengar, X. Li, J. M. Millam, G. A. Voth, G. E. Scuseria, and M. J. Frisch, *Ab initio* molecular dynamics: Propagating the density matrix with Gaussian orbitals. III. Comparison with Born–Oppenheimer dynamics, J. Chem. Phys. **117**, 8694 (2002).

[53] M. J. Frisch *et al.*, *Gaussian 16 Revision A.03* (Gaussian, Inc., Wallingford, CT, 2016).

[54] R. Wehlitz, P. N. Juranić, and D. V. Lukić, Double photoionization of magnesium from threshold to 54 eV photon energy, Phys. Rev. A **78**, 033428 (2008).

[55] M. Zawadzki, Electron-impact ionization cross section of formic acid, Eur. Phys. J. D **72**, 12 (2018).

[56] T. Nishimura, G. G. Meisels, and Y. Niwa, Bimodal kinetic energy release in the unimolecular dissociation of energy-selected formic acid ion, J. Chem. Phys. **91**, 4009 (1989).

[57] O. Vendrell, S. D. Stoychev, and L. S. Cederbaum, Generation of highly damaging H_2O^+ radicals by inner valence shell ionization of water, Chem. Phys. Chem. **11**, 1006 (2010).

[58] J. Zhou, C. He, M.-M. Liu, E. Wang, S. Jia, A. Dorn, X. Ren, and Y. Liu, Real-time observation of ultrafast molecular rotation in weakly bound dimers, Phys. Rev. Res. **3**, 023050 (2021).

[59] V. Stumpf, K. Gokhberg, and L. S. Cederbaum, The role of metal ions in x-ray-induced photochemistry, Nat. Chem. **8**, 237 (2016).

[60] G. Gopakumar, E. Muchová, I. Unger, S. Malerz, F. Trinter, G. Öhrwall, F. Lipparini, B. Mennucci, D. Céolin, C. Caleman, I. Wilkinson, B. Winter, P. Slavíček, U. Hergenhahn, and O. Björneholm, Probing aqueous ions with non-local Auger relaxation, Phys. Chem. Chem. Phys. **24**, 8661 (2022).

[61] T. Dudev and C. Lim, Principles governing Mg, Ca, and Zn binding and selectivity in proteins, Chem. Rev. **103**, 773 (2003).